Botts, Jonathan; Savioja, Lauri

Extension of a spectral time-stepping domain decomposition method for dispersive and dissipative wave propagation

Extension of a spectral time-stepping domain decomposition method for dispersive and dissipative wave propagation

Jonathan Botts[a)] and Lauri Savioja

Department of Computer Science, Aalto University, P.O. Box 11000, FI-00076 Aalto, Finland
jonathan.botts@aalto.fi, lauri.savioja@aalto.fi

Abstract: For time-domain modeling based on the acoustic wave equation, spectral methods have recently demonstrated promise. This letter presents an extension of a spectral domain decomposition approach, previously used to solve the lossless linear wave equation, which accommodates frequency-dependent atmospheric attenuation and assignment of arbitrary dispersion relations. Frequency-dependence is straightforward to assign when time-stepping is done in the spectral domain, so combined losses from molecular relaxation, thermal conductivity, and viscosity can be approximated with little extra computation or storage. A mode update free from numerical dispersion is derived, and the model is confirmed with a numerical experiment.
© 2015 Acoustical Society of America
[LT]
Date Received: June 16, 2014   **Date Accepted:** February 4, 2015

1. Introduction

Wave-based modeling for acoustic propagation requires a balance between computational efficiency, flexibility, and accuracy. Local methods for approximating solutions to partial differential equations, such as finite difference (FD) and finite element (FE) methods, offer flexibility and efficiency as they are based on local approximations or expansions of the solution on local bases. Spectral methods operate locally in a spectral domain and globally in a space-time domain, which typically leads to increased accuracy but also increased computational expense and decreased flexibility. For large models, local time-stepping methods tend to be memory-bound as opposed to compute-bound, while spectral approximations tend to shift the load toward computation and may require less memory if coarser discretization can be used without loss of accuracy.

In addition to formal order of accuracy, errors in time-domain FD, FE, and pseudospectral methods,[1,2] tend to affect the *phase* of a simulated response, to which human listeners may be sensitive. The prominence—and in some cases, the audibility—of these dispersion or phase errors determines usable bandwidth of a model. The point of departure for this letter will be the spectral domain-decomposition method in Refs. 3 and 4 because it combines isotropic propagation of pseudospectral methods[1,2] with dispersionless time-stepping. We will extend this method, previously used for the lossless linear wave equation,[3,4] to model frequency-dependent atmospheric attenuation and nonlinear dispersion relations.

2. Formulation

The description below is focused on the mode update aspect of the procedure in Refs. 3 and 4 which will be modified to approximate effects of atmospheric attenuation. The space-time solution is advanced in the modal domain as opposed to the time-domain

---

[a)]Author to whom correspondence should be addressed.

which allows for dispersionless updating. Subdomains are coupled as described in these references, so for brevity this aspect is omitted.

2.1 Lossless modal update

The solution of the wave equation in a cuboid cavity with rigid boundaries is well known. The eigenfunctions of the Laplacian, $\Phi(x)$, are Cosines and the time dependence is defined to be $e^{i\omega t}$, where $\omega = kc$, and $-k^2$ are eigenvalues of the Laplacian. To compute solutions in finite time with finite memory, the infinite sum of eigenfunctions is truncated. Indexed eigenfunctions, wave numbers, angular frequencies, and times are given by Φ_j, k_j, ω_j, t_n, respectively. The expanded solution is given by

$$\phi(x, t_n) = \sum_j u_j(t_n)\Phi_j(x). \tag{1}$$

Given this basis, the coefficients u_j may be computed in practice using a discrete Cosine transform (DCT). Given the above time-dependence for *modes* or modal coefficients, the time integration (updating, time-stepping, etc.) may be done exactly in the spectral domain. Each mode independently satisfies a harmonic oscillator equation. In addition, we admit a constant forcing term F_j.[3] Solutions are of the form

$$u_j^n = u_j(nT) = e^{i\omega_j nT} + F_j/\omega_j^2, \tag{2}$$

where u_j^n are again time-dependent modal coefficients, and $t = nT$. Given the solution at two adjacent time steps, it is possible to exactly update the solution to the next adjacent time step. The recursion relation may be derived from the sum of u^{n+1} and u^{n-1} for the non-forced oscillator or $(u^{n+1} - F/\omega^2)$ and $(u^{n-1} - F/\omega^2)$ for the forced oscillator, where the mode index has been suppressed. In discrete time-stepping form the modal update with forcing terms is given by[3,4]

$$u^{n+1} = 2\cos(\omega T)u^n - u^{n-1} + \frac{2F}{\omega^2}[1 - \cos(\omega T)]. \tag{3}$$

Note that at $\omega = 0$, the forcing term is undefined, but two applications of L'Hôpital's rule result in a forcing term $T^2 F$ at DC. If the DC forcing term is somehow neglected, the result is non-causal DC energy introduced to or from neighboring domains. It is also interesting to note that this update is nearly identical to leapfrog time integration except that the central coefficient is frequency dependent. One can see how a frequency-independent coefficient, as would be used with typical pseudospectral time-stepping,[1,2] should introduce frequency-dependent propagation errors.

The mode update involves computing modal coefficients u_j through the DCT and applying Eq. (3) to each mode. Then, the updated space-time solution is used to compute forcing terms with finite difference approximations.[3,4] The forcing terms are then transformed to the modal domain and introduced to the solution as F_j in Eq. (3).

2.2 Lossy modal update

The point of departure for modeling losses due to viscosity and thermal conductivity is the lossy wave equation,[5]

$$\frac{1}{c^2}\frac{\partial^2}{\partial t^2}\phi(x, t) = \left(1 + \tau\frac{\partial}{\partial t}\right)\nabla^2\phi(x, t), \quad \tau = \frac{((4/3)\eta + \eta_B)}{\rho_0 c^2}, \tag{4}$$

where τ is a relaxation time depending on shear viscosity η and bulk viscosity η_B of the medium.[5] This equation with constant relaxation time has been used to approximate viscous losses in time-domain FD models,[6,7] and to introduce more flexible frequency-dependence other terms have been heuristically added as well.[6] The relaxation time may be assigned based solely on viscosity or the classical absorption coefficient which also approximates losses from thermal conductivity.[5]

Equation (4) may be reduced to a lossy Helmholtz equation, but in order to compute modal coefficients with the DCT, solutions should again be of the form $\phi(x,t) = U(t)\Phi(x)$, where $\Phi(x)$ are eigenfunctions of the undamped Laplacian. Let $-k^2$ be the eigenvalues of the undamped Laplacian, as above. With these definitions, Eq. (4) reduces to a damped harmonic oscillator equation,

$$U''(t) + \tau c^2 k^2 U'(t) + c^2 k^2 U(t) = 0. \tag{5}$$

Now, let $U(t) = e^{-\alpha t}\, e^{i\omega t} = e^{(i\omega - \alpha)t}$, where mode indices are again suppressed. Substitution into Eq. (5) results in

$$(\alpha^2 - \omega^2 - \alpha\tau c^2 k^2 + c^2 k^2) + i(\tau c^2 k^2 \omega - 2\omega\alpha) = 0, \tag{6}$$

where real and imaginary terms have been grouped. All variables are assumed to be real, so for non-trivial solutions the real and complex terms must vanish independently. With $\omega_0 \equiv ck$, these two equations lead to

$$\alpha = \frac{\tau c^2 k^2}{2} = \frac{\tau \omega_0^2}{2}, \quad \omega^2 = \omega_0^2\left(1 - \frac{\alpha^2}{\omega_0^2}\right) = \omega_0^2\left(1 - \frac{\tau^2\omega_0^2}{4}\right). \tag{7}$$

When $\tau \to 0$, the limit of the lossless case, $\alpha \to 0$ and $\omega^2 \to \omega_0^2$. It is also straightforward to confirm that the solution with constant forcing is $U(nT) = e^{(i\omega - \alpha)t} + F/\omega^2$. For a frequency-independent relaxation time τ, the absorption coefficient α is defined by Eq. (7). Note that this is a temporal absorption coefficient, while atmospheric attenuation is often reported as a function of distance.[8]

The recursion relation is computed in a similar way to Eq. (3). For solutions of the form $V^n = U^n - F/\omega^2 = e^{(i\omega - \alpha)nT}$, the sum of V^{n+1} and $e^{-2\alpha T}\,V^{n-1}$ leads to the update for modal coefficients

$$U^{n+1} = 2e^{-\alpha T}\cos(\omega T)U^n - e^{-2\alpha T}U^{n-1} + \frac{F}{\omega^2}\left[1 + e^{-2\alpha T} - 2\cos(\omega T)\right]. \tag{8}$$

The forcing term at DC ($\omega = 0$) is again $T^2 F$. Since $\Phi(x)$ are defined to be eigenfunctions of the Laplacian, the DCT can still be used to transform to the spectral domain. In this way, viscous losses may be modeled with the framework in Ref. 3 simply by updating modes with Eq. (8) instead of Eq. (3).

2.3 Memory usage

In time-domain finite difference methods, adding the viscous term requires storing one extra value per grid node—an increase from two values per node to three values per node.[6,7] The attenuation described above entails either re-computation of coefficients or storage of one more value per grid node. In its minimal configuration with no stored coefficients, there are five necessary field values, one of which may be re-used, resulting in four required values per node. However, depending on the balance of memory access and computation, it may be advantageous to precompute coefficients and store them, increasing the base memory requirement. One could, for instance, store the four requisite field values in addition to the coefficients multiplying u_j^n and F_j in Eq. (3) or U^n, U^{n-1}, and F^n in Eq. (8)—requiring six and seven values per node, respectively. One could also store ω_j and α_j in Eq. (8)—requiring six values per node—and partially compute coefficients for each iteration. The additional memory requirement for the spectral formulation should be either zero or one extra value per node over an analogous implementation of the lossless update.

2.4 Frequency-dependent atmospheric attenuation

The procedure for assigning frequency-dependence to the absorption coefficient $\alpha \equiv \alpha(\omega)$ or relaxation time $\tau(\omega)$ is relatively straightforward given Eq. (8). The absorption coefficient is simply assigned individually to each mode, just as the other

coefficients in the update are. Consider the model for atmospheric attenuation $\tilde{\alpha}(x,f)$ in Ref. 8, a function of temperature, atmospheric pressure, relative humidity, distance, and frequency f in hertz. Note that other derivative quantities, such as relaxation frequencies for oxygen and nitrogen, are computed from these values. The absorption coefficient in Eq. (8) is a temporal damping coefficient, so the output of the model in Ref. 8 should be scaled such that $\alpha_j = \tilde{\alpha}(f_j)c_0/(2\pi)^2$. The accuracy of this assignment is confirmed in the following section.

2.5 Frequency-dependent wave speed

Just as frequency-dependent dissipation may be assigned individually to each mode, frequency-dependent wave speed may be assigned to model dispersive wave propagation by letting $\omega_j = c_j k_j$, where c_j is the phase speed associated with the jth mode. For instance, assigning $c_j = k_j$ results in the solution to the bending wave equation $u_{tt} + \nabla^2\nabla^2 u = 0$, where subscripts indicate partial derivatives. This results in $\omega_j = k_j^2$, which may be substituted into Eq. (3). Other relatively arbitrary dispersion relations may be assigned in the same way; however, large variations in wave speed may restrict the size of the time step. Interfacing also need not change since the solution is still expanded on the Cosine basis.

3. Numerical Experiments

The following experiments are intended to evaluate and confirm the implementation of frequency dependent attenuation and dispersive propagation. The source of numerical errors with this approach is interfacing, so without interfaces, there are no numerical errors to expect except those due to rounding. There may be errors orthogonal to the finite Cosine basis such as frequency components higher than what can be resolved. All external boundaries for the simulated spaces have homogeneous Neumann boundary conditions for simplicity, which are implicit in the Cosine basis.

3.1 Interface errors

To provide context for the following experiments, we show numerically measured interface errors, characterized by reflection and transmission coefficients, at normal incidence for interfaces of orders 2–8 in Fig. 1. The domain is excited by a unit-amplitude plane wave at a single plane of nodes. This is therefore the maximum bandwidth which can be expected for the chosen time step, in this case $T = X/2c$. An ideal interface would show complete transmission (0 dB) and no reflection.

3.2 Atmospheric attenuation

To evaluate the atmospheric attenuation model, we examine plane wave propagation in rectangular tubes with rigid boundaries. Each experiment is done in a single-domain
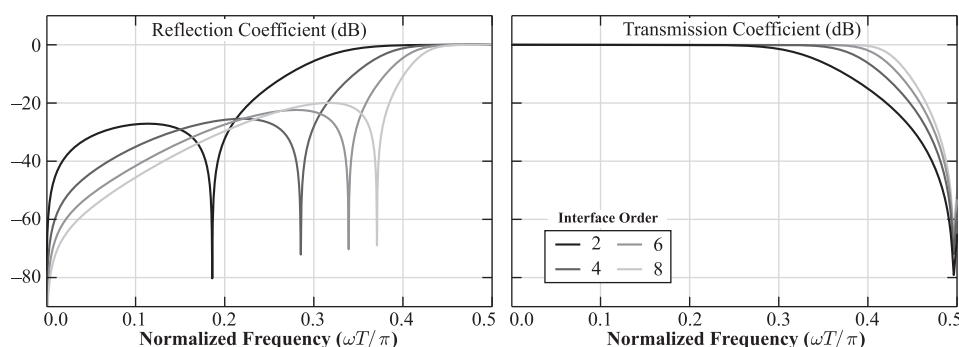

Fig. 1. Empirical reflection and transmission coefficients for a plane wave at normal incidence upon an interface of the indicated order. For this choice of time step, there is virtually no energy above half the Nyquist frequency, $\omega T = \pi/2$.

tube of length $L = 2048$ nodes, with 8×8-node cross-section, and a unit-impulse plane-wave excitation at one end. Since the excitation is a plane wave and the model does not account for losses in the boundary layer, the cross-sectional area is not important. Two experiments are used to evaluate performance in both low and high frequency ranges. The normalized dimensions of each model are the same, but the largest dimension is scaled to 50 and 0.5 m, respectively. The time-step is set to $T = X/(1.15c_0)$, slightly below the one-dimensional stability limit, where X is the spatial discretization step. Pressure signals used to compute attenuation are recorded at distances 683 and 1365 nodes from the end of the tube, approximately $L/3$ and $2L/3$. In this scenario, there should be no losses in amplitude except due to atmospheric attenuation.

Figure 2 shows theoretical and measured attenuation for various attenuation models. The frequency-independent classical absorption coefficient $\alpha_c/\omega^2 = 1.37 \times 10^{-11} c_0/(2\pi)$,[2] approximating losses from viscosity and thermal conductivity in air at 20 °C, is taken from Table 8.5.1 in Ref. 5. The other curves correspond to the model in Ref. 8 with relative humidities varying from 0% to 100% in 20% increments. The measured attenuation in the highest and lowest frequency bins contain errors, but piecing together results from both tubes at 4×10^3 Hz. produces suitable broadband result. Figure 2 may be compared to Fig. 1 in Ref. 8.

This experiment confirms the implementation more than it quantifies numerical errors since there are no numerical errors to expect beyond rounding errors and those orthogonal to the finite Cosine basis. It is also worth emphasizing that this is not strictly speaking a physical approximation to the various loss mechanisms. A full non-linear physical model would also account for losses near boundaries as well as convective terms. However, for the purposes of room acoustics and environmental acoustics, assigning frequency-dependent damping in the free field should sufficiently approximate the important effects for most problems.

3.3 Dispersive propagation

This series of experiments is done in a three-dimensional rectangular geometry which is artificially divided into subdomains with vertical symmetry for simplicity. The
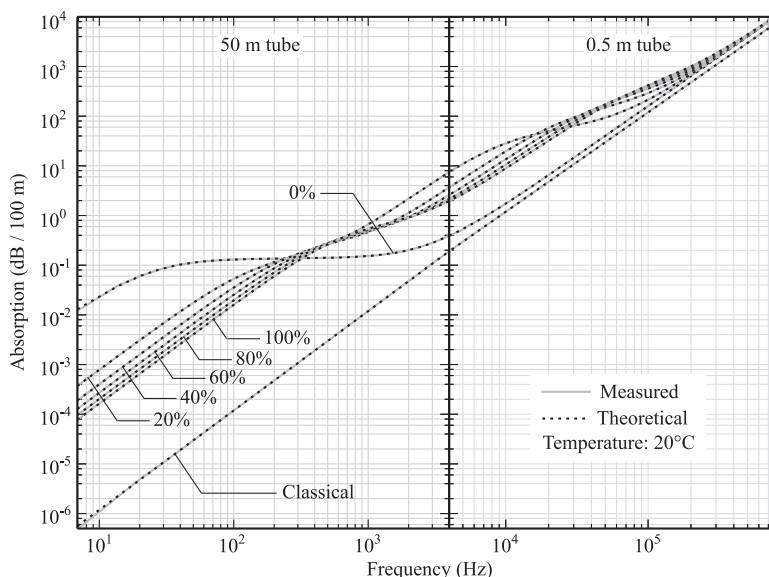

Fig. 2. Confirmation of the frequency-dependent air absorption model, based on Ref. 8. The absorption coefficient in Ref. 8 is scaled by $c_0/(2\pi)^2$ when used with Eq. (8). Percentages indicate the relative humidity used in the model.

simulations summarized by the video in Mm. 1 show both non-dispersive and dispersive wave propagation.

> Mm. 1. Demonstration of dispersive propagation and coupling between dispersive and non-dispersive subdomains (11.4 MB).

The initial condition is a narrow Gaussian pulse, and modes are updated with Eq. (3). Interfacing is done with sixth-order finite difference approximations to the Laplacian where coefficients are generated using the method of undetermined coefficients.[9]

The first condition demonstrates dispersionless propagation with wave speed $c_0 = 1$. Interfacing errors are not visible in this condition but are nevertheless present. The second condition uses wave speed $c_j = c_0 \, k_j$, so high frequencies travel faster than lower frequencies. The maximum wave speed is $c_{max} = c_0\sqrt{3\pi}/h$. The first dispersive example uses only a single subdomain to show the solution in the absence of interfacing errors, and the second dispersive example uses the decomposed domain to show the effect of interfacing errors. Since high-frequency components are spatially and temporally separated from low-frequency components, the predominently high-frequency interfacing errors are much more apparent. The fourth condition uses wave speed $c_j = c_0 k_j^{-1/2}$, which causes low frequencies to travel faster than high frequencies.

The final example demonstrates coupling between dispersive and non-dispersive subdomains. The dispersive subdomain is assigned wave speed $c_j = c_0 \, k_j$, and the non-dispersive subdomain is assigned wave speed $c_j = c_{max}/6 = \text{const}$. The interfacing is unchanged from the procedure in Ref. 3 and still maintains continuous solutions across the interface. Waves incident upon the dispersive material are reflected, and wavefronts diffract and scatter from corners as expected. These wave speeds and dispersion relations are not intended to correspond to specific physical systems but to demonstrate the straightforward application of nonlinear dispersion relations and coupling of different media.

4. Conclusions

The spectral domain-decomposition method in Refs. 3 and 4 was extended to include atmospheric attenuation and dispersive wave speeds with arbitrary frequency dependence. The model requires only a small amount of extra computation over the lossless, dispersionless formulation, while retaining dispersionless time-stepping in the modal domain. The attenuation model was evaluated with a numerical experiment in Sec. 3.2 with agreement up to numerical accuracy. The video in Mm. 1 demonstrates dispersive propagation as well as coupling between dispersive and non-dispersive media. Future work could address a number of topics including formulation of physically motivated boundary conditions, thorough evaluation of stability and interfacing errors, as well as other approaches to interfacing subdomains.

Acknowledgments

References and links

[1]B. Fornberg, *A Practical Guide to Pseudospectral Methods, Cambridge Monographs on Applied and Computational Mathematics* (Cambridge University Press, Cambridge, UK, 1998), 233 pp.

[2]M. Hornikx, R. Waxler, and J. Forssén, "The extended Fourier pseudospectral time-domain method for atmospheric sound propagation," J. Acoust. Soc. Am. **128**, 1632–1646 (2010).

[3]N. Raghuvanshi, R. Narain, and M. Lin, "Efficient and accurate sound propagation using adaptive rectangular decomposition," IEEE Trans. Vis. Comp. Graphics **15**, 789–801 (2009).

[4]R. Mehra, N. Raghuvanshi, L. Savioja, M. Lin, and D. Manocha, "An efficient GPU-based time domain solver for the acoustic wave equation," Appl. Acoust. **73**, 83–94 (2012).

[5]L. Kinsler, A. Frey, A. Coppens, and J. Sanders, *Fundamentals of Acoustics* (Wiley, Hoboken, NJ, 1999), pp. 210-224.

[6]C. de Groot-Hedlin, "Finite-difference time-domain synthesis of infrasound propagation through an absorbing atmosphere," J. Acoust. Soc. Am. **124**, 1430–1441 (2008).

[7]C. Webb and S. Bilbao, "Computing room acoustics with CUDA - 3D FDTD schemes with boundary losses and viscosity," in *IEEE International Conference on Acoustics, Speech, Signal Processing* (2011), pp. 317–320.

[8]H. Bass, L. Sutherland, A. Zuckerwar, D. Blackstock, and D. Hester, "Atmospheric absorption of sound: Further developments," J. Acoust. Soc. Am. **97**, 680–683 (1995).

[9]J. W. Thomas, *Numerical Partial Differential Equations: Finite Difference Methods* (Springer-Verlag New York, 1995), Vol. 22, pp. 19–21.